

# Some Topics of Isoscalar Spin-triplet Pairing

YKIS2022, June 8, 2022

Hiroyuki Sagawa RIKEN/University of Aizu

1. Introduction
2. Competition between  $(S=1, T=0)$  and  $(S=0, T=1)$  pairing correlations
3. Energy spectra of  $N=Z$  nuclei
4. Gamow-Teller giant resonances in  $N=Z+2$  nuclei and  $SU(4)$  supermultiplet
5. Role of Isoscalar Pairing on pair transfer reaction
6. Double beta-decay
7. Summary



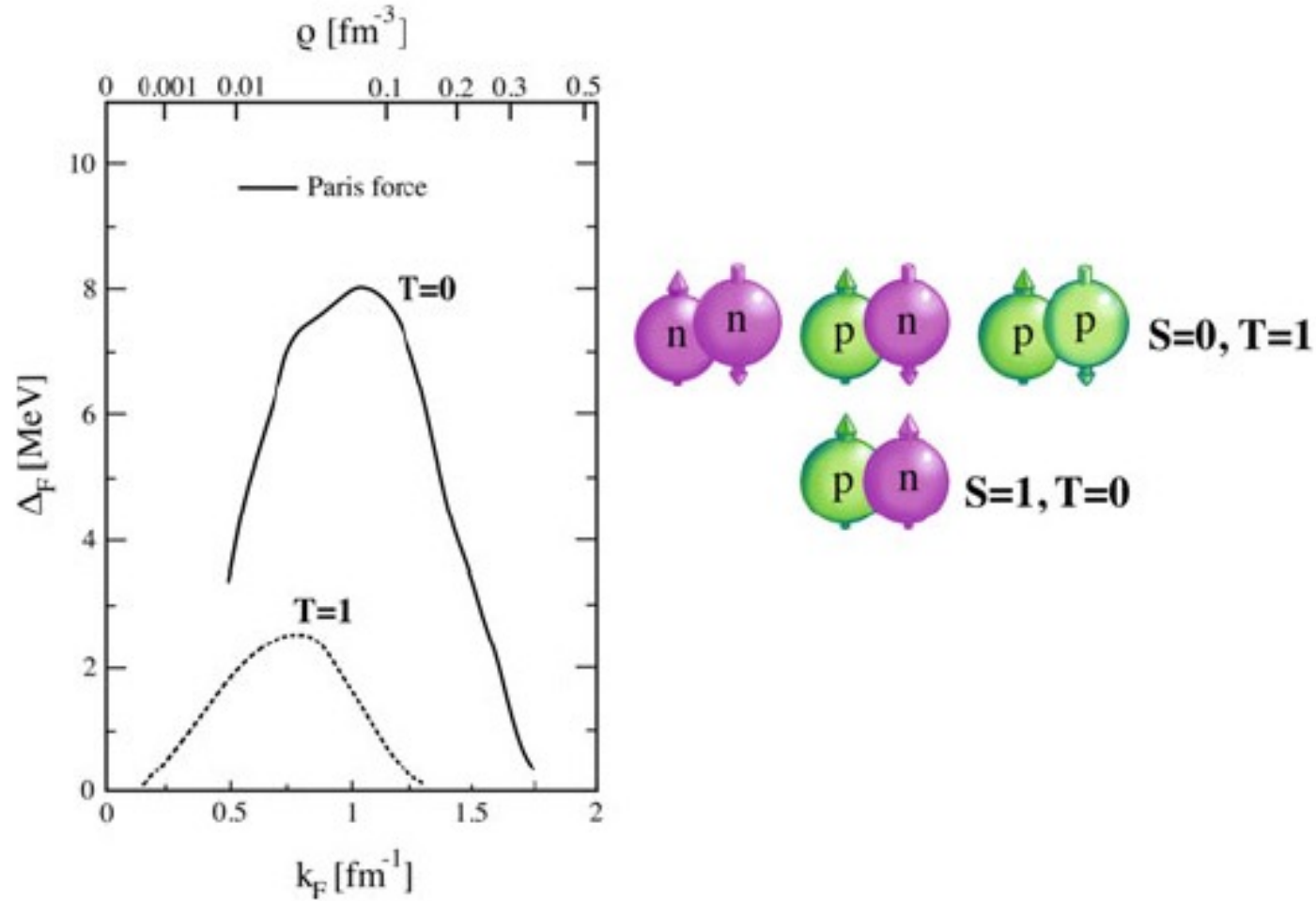


**Fig. 6.52** Fermi momentum dependence of the pairing gaps in symmetric nuclear matter, for the  $T = 0$  spin-triplet and the  $T = 1$  spin-singlet channels calculated by using the Paris potential. The corresponding nuclear density is also given in the upper axis of the figure for the  $T = 0$  case. Figure reprinted with permission from [50]. ©2021 by the American Physical Society

E. Garrido et al., Phys. Rev. C **63**, 037304 (2001)

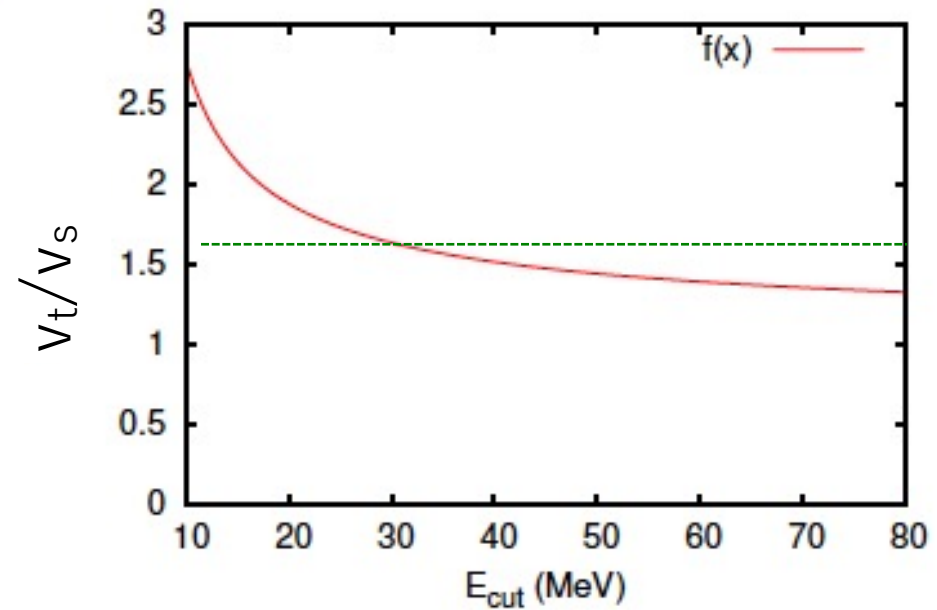
# pn pairing interaction (HFB, Three-body model)

$$V_{np}(\mathbf{r}_1, \mathbf{r}_2) = \hat{P}_s v_s \delta(\mathbf{r}_1 - \mathbf{r}_2) \left[ 1 + x_s \left( \frac{\rho(r)}{\rho_0} \right)^\alpha \right] \\ + \hat{P}_t v_t \delta(\mathbf{r}_1 - \mathbf{r}_2) \left[ 1 + x_t \left( \frac{\rho(r)}{\rho_0} \right)^\alpha \right]$$

$$\hat{P}_s = \frac{1}{4} - \frac{1}{4} \boldsymbol{\sigma}_p \cdot \boldsymbol{\sigma}_n, \quad \hat{P}_t = \frac{3}{4} + \frac{1}{4} \boldsymbol{\sigma}_p \cdot \boldsymbol{\sigma}_n.$$

$$v_s = \frac{2\pi^2 \hbar^2}{m} \frac{2a_{pn}^{(s)}}{\pi - 2a_{pn}^{(s)} k_{\text{cut}}},$$

$$v_t = \frac{2\pi^2 \hbar^2}{m} \frac{2a_{pn}^{(t)}}{\pi - 2a_{pn}^{(t)} k_{\text{cut}}},$$



Scattering length

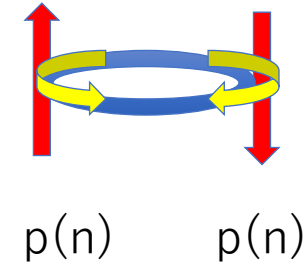
$$a_{pn}^{(s)} = -23.749 \text{ fm and } a_{pn}^{(t)} = 5.424 \text{ fm}$$

$$E_{\text{cut}} = k_{\text{cut}}^2 / 2m$$

## Two particle systems

T=1, S=0 pair

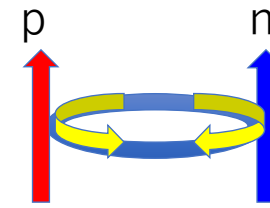
$$|(L = S = 0)J = 0, T = 1\rangle \Rightarrow |(j = j')J = 0, T = 1\rangle$$



T=0, S=1 pair

$$|(L = 0, S = 1)J = 1, T = 0\rangle \Rightarrow$$

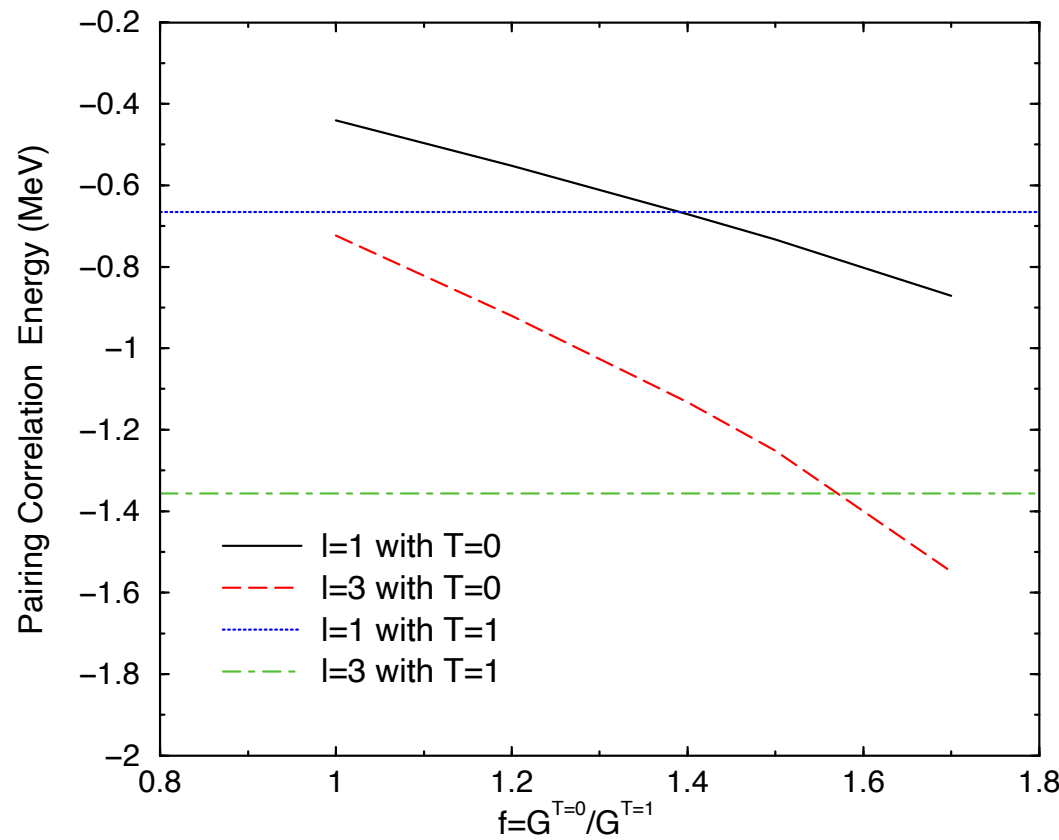
$$a|(l = l' j = j')J = 1, T = 0\rangle + b|((l = l')j, j' = j \pm 1)J = 1, T = 0\rangle$$



Single-particle wave function:  $\vec{j} = \vec{l} + \vec{s}$

The total wave function should be anti-symmetric in spin-isospin-relative angular momentum quantum space.

If there is strong spin-orbit splitting, it is difficult to make (T=0, S=1) pair.



Pairing correlation energy of  $(J,T)=(0,1)$  and  $(1,0)$  states in  $pf$  shell

Even with large spin-orbit splitting for  $f$ -orbits, the spin-triplet correlations will be larger than the spin-singlet one for  $f > 1.5$

HS, Y. Tanimura and K. Hagino, PRC87, 034310 (2013)

G.F. Bertsch and Y. Luo, PRC81, 064320 (2010)

**TABLE I. Strengths of triplet and singlet interactions from shell-model fits and their ratios. See text for details.**

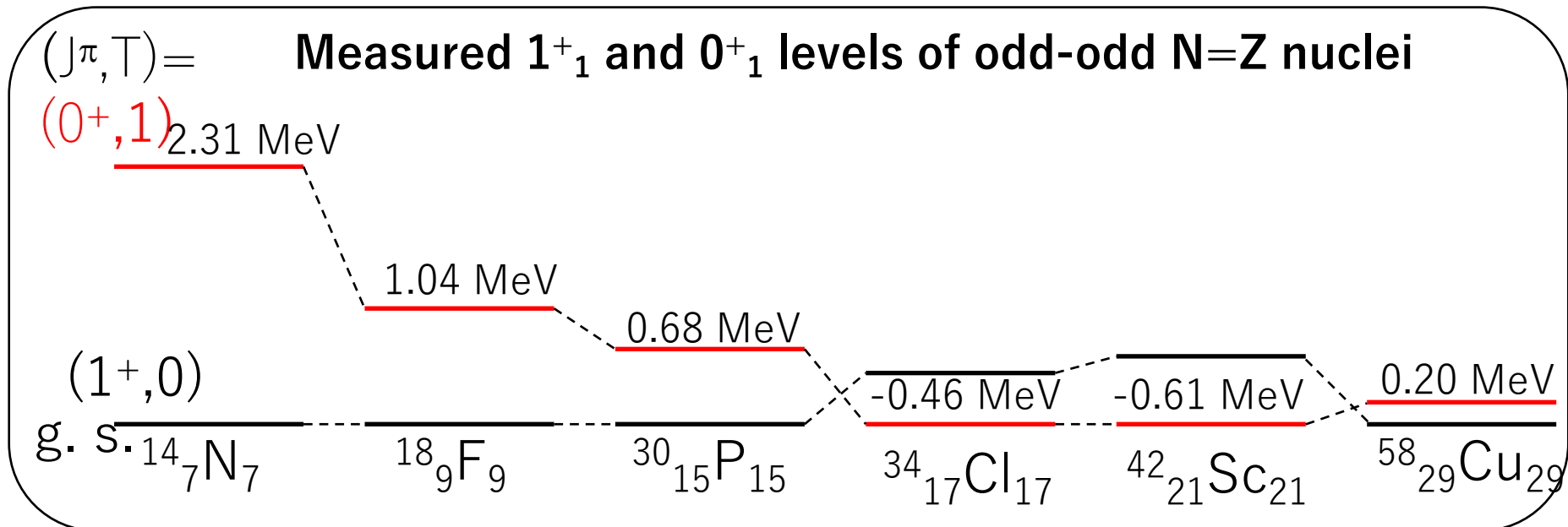
Source	$v_s$ (MeV fm <sup>3</sup> )	$v_t$ (MeV fm <sup>3</sup> )	Ratio
<i>sd</i> shell [8]	280	465	1.65
<i>fp</i> shell [9]	291	475	1.63

# N=Z odd-odd nuclei with 3-body model

Y. Tanimura, HS, K. Hagino,  
PTEP 053D02 (2014)

- n-p pairing interactions
  - ✓ We have two channels  $T=0$  and  $1$
  - ✓  $T=0, S=1$  is attractive stronger than  $T=1, S=0$  pair  
cf. deuteron, matrix elements in shell models
  - ✓ The strong spin-orbit coupling  
may quench or even kill  $T=0$  pairing

when the angular momentum is larger, the spin-orbit is larger  
and  $T=0$  pair correlations decrease



# Three-body Model

## Total 3-body Hamiltonian

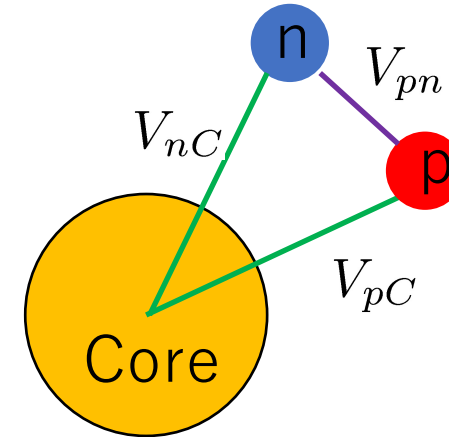
$$H = \frac{\mathbf{p}_p^2}{2m} + \frac{\mathbf{p}_n^2}{2m} + V_{pC}(\mathbf{r}_p) + V_{nC}(\mathbf{r}_n) \\ + V_{pn}(\mathbf{r}_p, \mathbf{r}_n) + \frac{(\mathbf{p}_p + \mathbf{p}_n)^2}{2A_C m}$$

## Core-N mean field

$$V_{(p/n)C}(r) = v_0 f(r) + v_{ls} \frac{1}{r} \frac{d}{dr} f(r) (\mathbf{l} \cdot \mathbf{s}) (+Coulomb) \\ f(r) = \frac{1}{1 + e^{(r-R)/a}}$$

## p-n interaction

$$V_{pn} = \hat{P}_s v_s \delta(\mathbf{r}_p - \mathbf{r}_n) \left[ 1 + x_s \left( \frac{\rho(r)}{\rho_0} \right)^\alpha \right] \\ + \hat{P}_t v_t \delta(\mathbf{r}_p - \mathbf{r}_n) \left[ 1 + x_t \left( \frac{\rho(r)}{\rho_0} \right)^\alpha \right]$$



Determination of parameters

$v_0, v_{ls}$ : neutron separation energy

$v_s, v_t$ : pn scattering length with  $E_{\text{cut}} (= 20 \text{ MeV})$   $\Rightarrow$

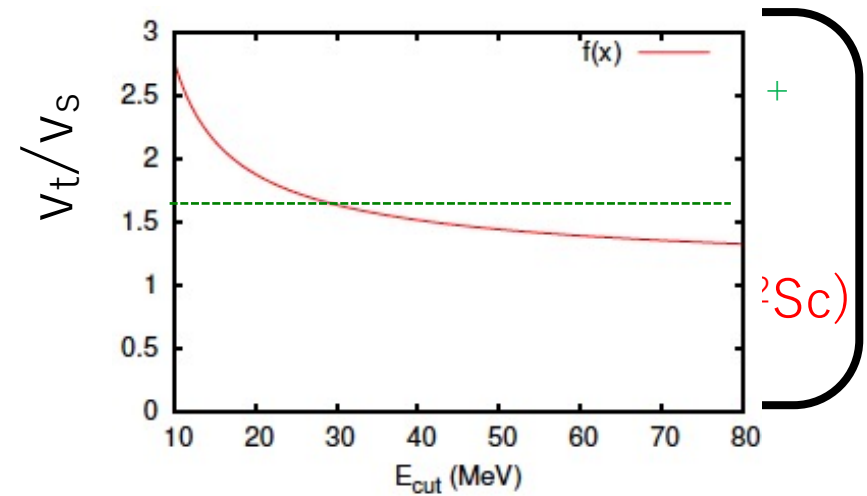
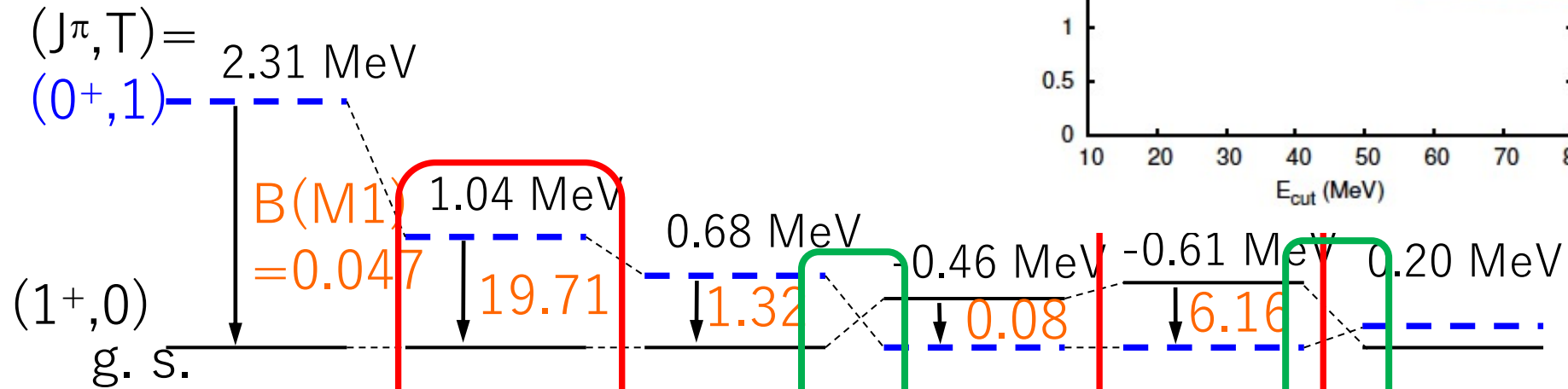
$v_s/v_t = 1.7$  (spin-triplet pairing is much stronger than spin-singlet)

$x_s, x_t, \alpha$ :  $1^+, 3^+, 0^+$  in  $^{18}\text{F}$  energies are fitted

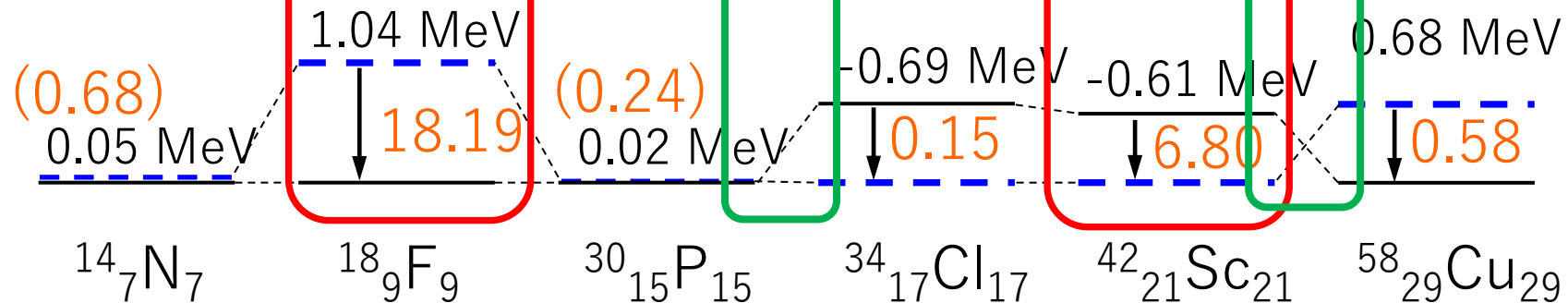
Diagonalization in a large model space

# 1. $E_{0^+} - E_{1^+}$ and $B(M1)$

(a) Experiment [/www.nndc.bnl.gov](http://www.nndc.bnl.gov)



(b) Three-body model



The inversion of  $1^+$  and  $0^+$  shows a clear manifestation of the competition between spin-orbit and the spin-triplet pairing.



results

## $^{18}\text{F}$ and $^{42}\text{Sc}$ : large B(M1)

Separate Contribution to  $\langle f || O(M1) || i \rangle (\mu_N)$

	$^{14}\text{N}$	$^{18}\text{F}$	$^{30}\text{P}$	$^{34}\text{Cl}$	$^{42}\text{Sc}$	$^{58}\text{Cu}$
Valence orbital	p1/2	d5/2	s1/2	d3/2	f7/2	p3/2
orbital	1.09	<b>1.28</b>	0.21	2.28	<b>2.91</b>	0.09
$g_s^{IV} \sum \tau_3(i) s(i)$	-2.78	<b>7.44</b>	-1.21	-3.65	<b>6.34</b>	<b>1.47</b>
$g_s^{IS} \sum_i s(i)$	$5 \times 10^{-5}$	$3 \times 10^{-3}$	$3 \times 10^{-5}$	$-1 \times 10^{-4}$	$2 \times 10^{-3}$	$-2 \times 10^{-3}$
B(M1) ↓ ( $\mu_N^2$ )	0.047	19.71	1.32	0.08	6.16	---
Exp.						
Calc.	0.68	<b>18.19</b>	0.24	0.15	<b>6.80</b>	0.58

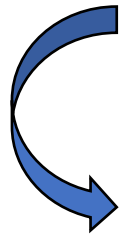
- ✓  $(j=l-1/2)^2$  spin and orbital are cancelled  
(Lisetskiy et al., PRC60, 064310 ('99))  $\Rightarrow$   $^{14}\text{N}, ^{34}\text{Cl}$  B(M1) **small**
- ✓  $(j=l+1/2)^2$  spin and orbital coherent  
(Lisetskiy et al., PRC60, 064310 ('99))  $\Rightarrow$   $^{18}\text{F}, ^{42}\text{Sc}$  B(M1) **large**
- ✓ good SU(4) symmetry
- ✓ even  $j=l+1/2$  not good SU(4) symmetry  $\Rightarrow$   $^{58}\text{Cu}$  B(M1) **small**

# Results

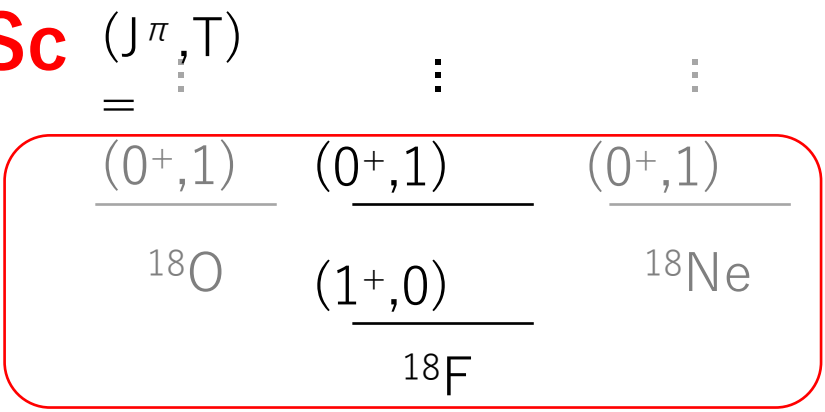
## Large B(M1) in $^{18}\text{F}$ and $^{42}\text{Sc}$ $(J^\pi, T)$

$^{18}\text{F}$  :

$$\left\{ \begin{array}{l} 1^+ \rightarrow P(S=1) = 90.1\%, (1d)^2 \\ 0^+ \rightarrow P(S=0) = 82.2\%, (1d)^2 \end{array} \right.$$



1<sup>+</sup> and 0<sup>+</sup> can be considered as the states in the same SU(4) multiplets (LST) = (0,1,0), (0,0,1)  
The same as  $^{42}\text{Sc}$  in 1f-orbits

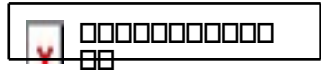
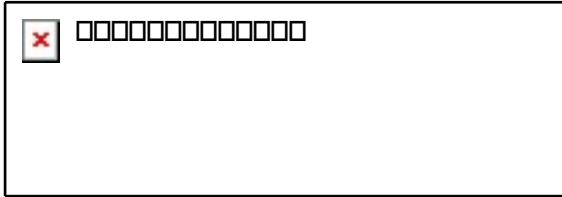


SU(4 multiplet)

$$O(M1) \propto \sum_i [g_s(i)s(i) + g_\ell(i)\ell(i)]$$

$$= \underbrace{g_s^{IV}}_{\text{Large}} \sum_i \tau_3(i)s(i) + \underbrace{g_s^{IS}}_{\text{(small)}} \sum_i s(i) + \sum_i g_\ell(i)\ell(i)$$

SU(4) generator



Gamow-Teller Transitions in nuclei with  $N=Z+2$   
C.L. Bai, HS, G. Colo, Y. Fujita et al.,

PRC90, 054335 (2014)

HFB+QRPA with  $T=1$  and  $T=0$   
pairing  
 $T=1$  pairing in HFB  
 $T=0$  pairing in QRPA

$$\hat{O}(GT) = \sigma\tau_{\pm}$$

$\sigma$ ,  $\tau$  and  $\sigma\tau$  are generators of SU(4)

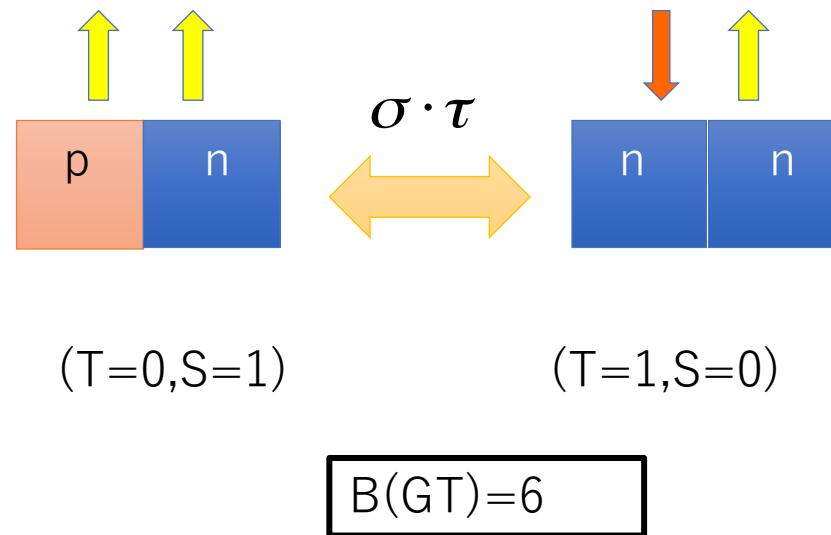
Supermultiplet : Wigner SU(4) symmetry  
(E. Wigner 1937, F. Hund 1937)  
( $T=1, S=0$ )  $\rightarrow$  ( $T=0, S=1$ ) GT transition is allowed and enhanced .

$$V_{T=1}(\mathbf{r}_1, \mathbf{r}_2) = V_0 \frac{1 - P_{\sigma}}{2} \left(1 - \frac{\rho(\mathbf{r})}{\rho_0}\right) \delta(\mathbf{r}_1 - \mathbf{r}_2), \quad (1)$$

$$V_{T=0}(\mathbf{r}_1, \mathbf{r}_2) = fV_0 \frac{1 + P_{\sigma}}{2} \left(1 - \frac{\rho(\mathbf{r})}{\rho_0}\right) \delta(\mathbf{r}_1 - \mathbf{r}_2), \quad (2)$$

Supermultiplet : Wigner SU(4) symmetry  
(T=1, S=0)  $\rightarrow$  (T=0, S=1) GT transition is allowed and enhanced .

Spacial symmetry is the same between the initial and final states



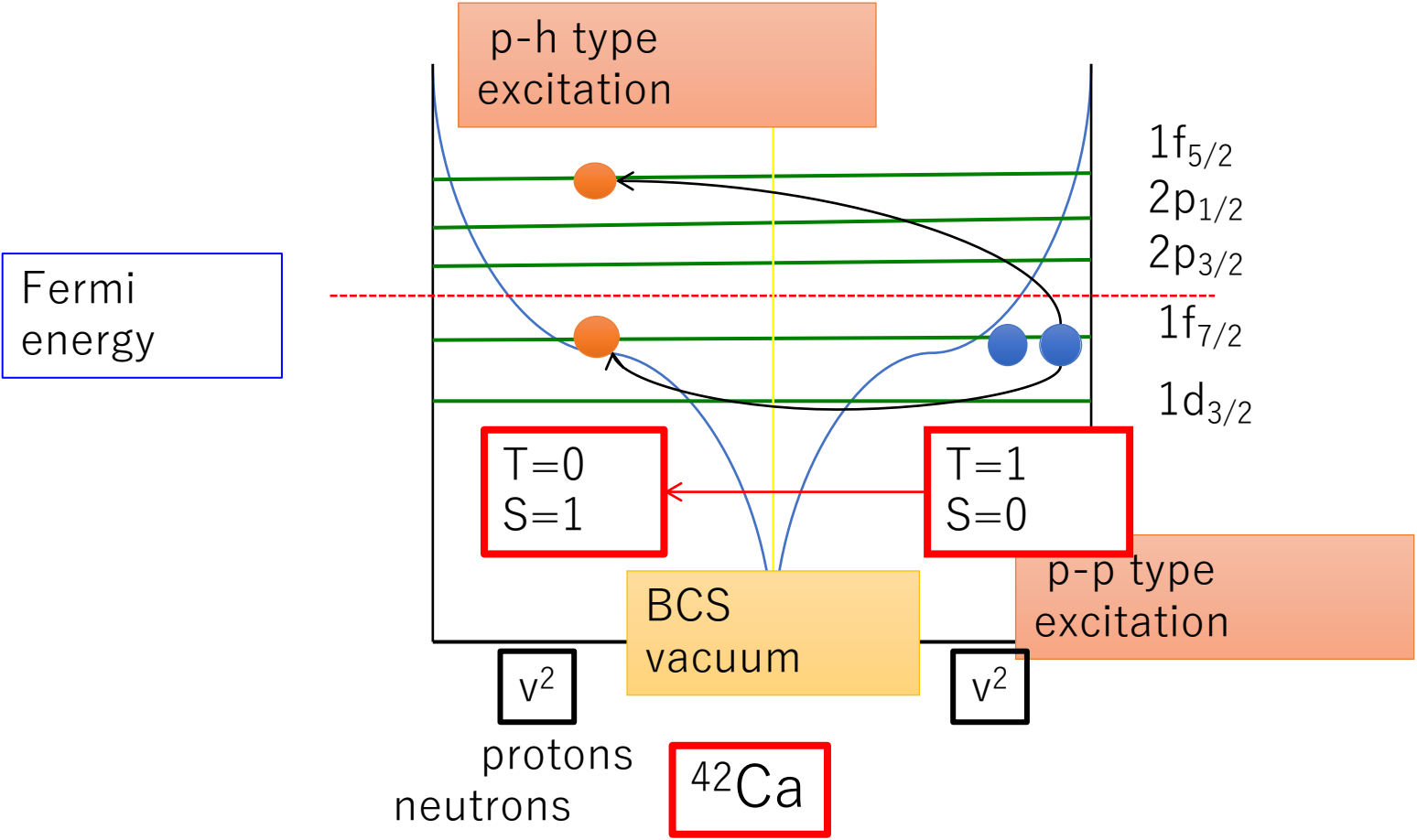
Well-known in light p-shell nuclei (LS coupling dominance)

What happens in **pf shell nuclei** with strong spin-orbit and spin-triplet pairing interactions?

Gamow-Teller transitions in  $N=Z+2$   $pf$  nuclei

Gamow-Teller transitions in BCS vacuum

$$\hat{O}(GT) = \sigma\tau_{\pm}$$

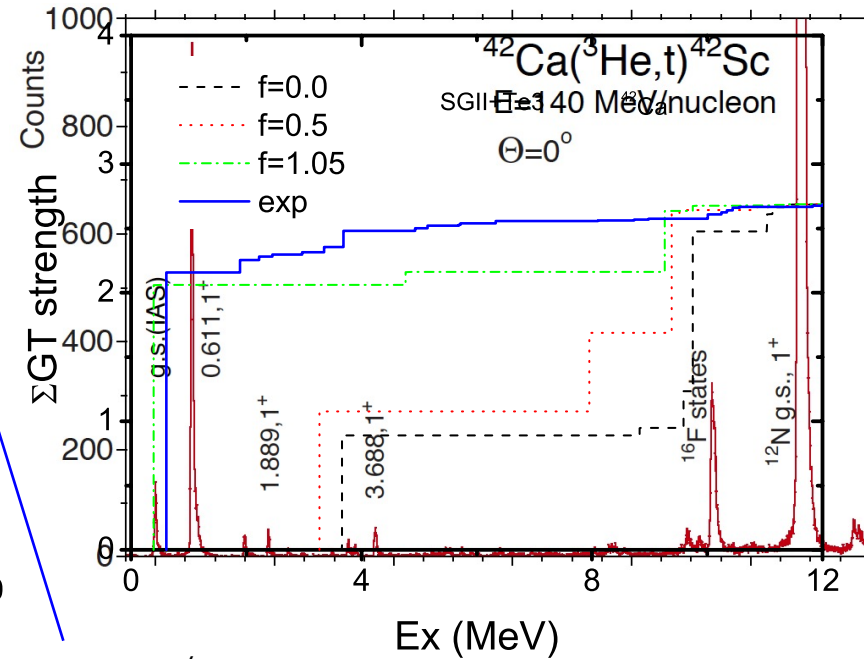
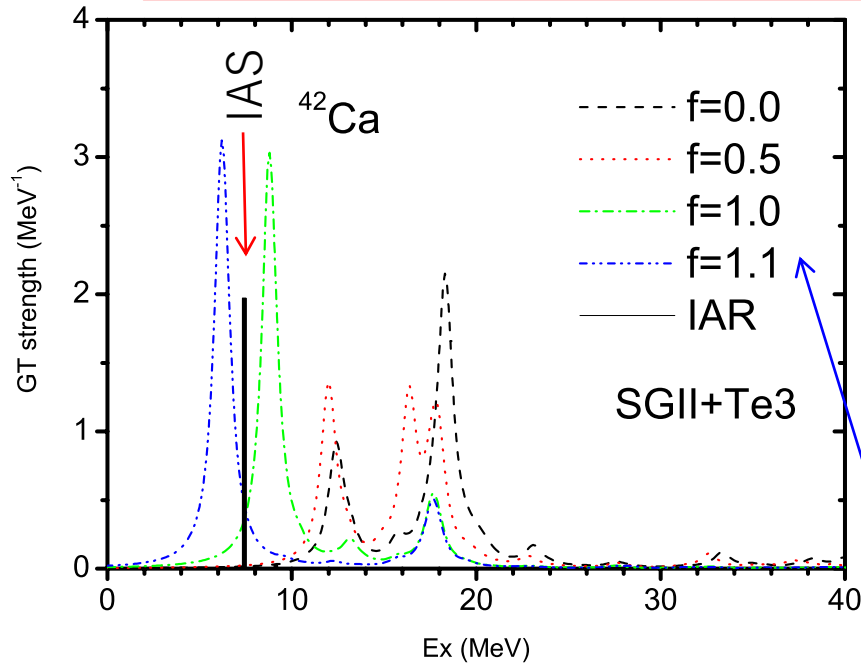


Fermi energy

A pair of  $SU(4)$  supermultiplet

Spin-spin is  $T=0$  interaction, attractive and spin-down  $\rightarrow$  Higher energy  
 Collective Gamow-Teller states.

$\rightarrow$  SU(4) symmetry restoration



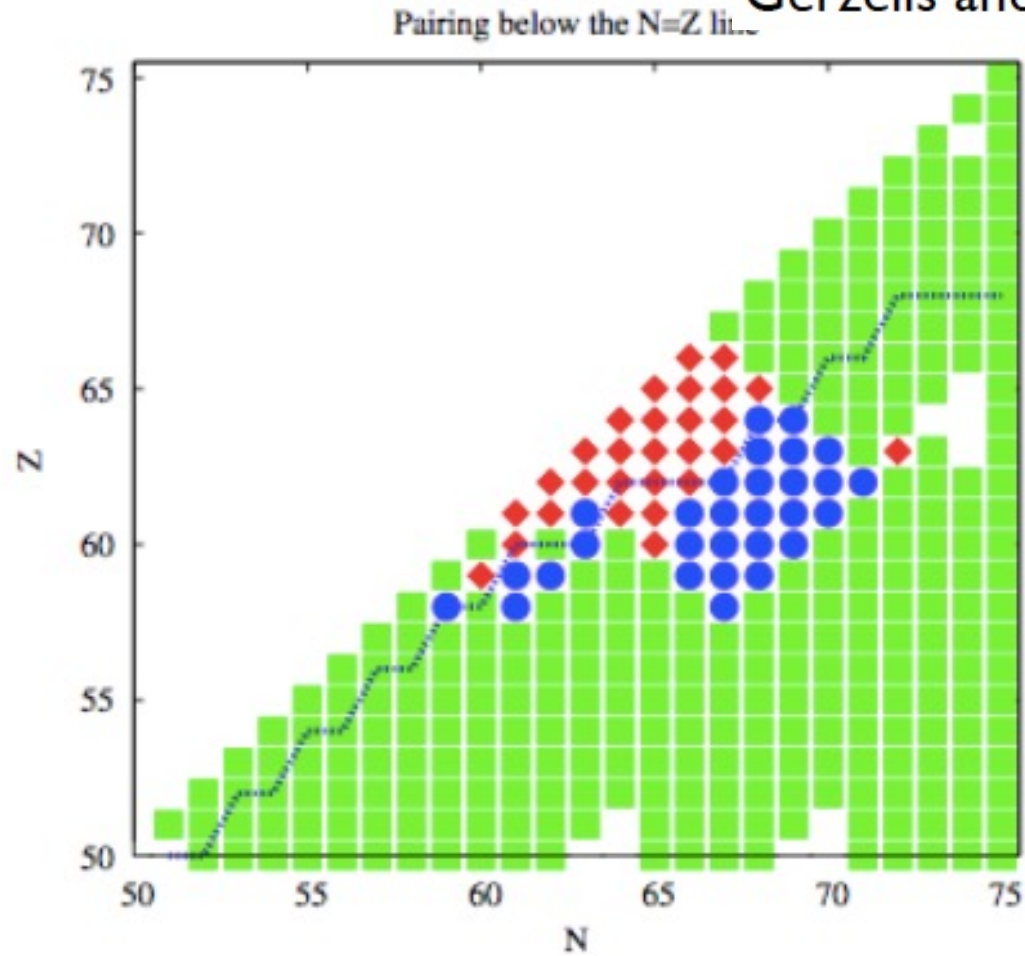
$f = \text{IS/IV}$   
pairing

HFB+QRPA with  $T=1$  and  $T=0$  pairing

$T=0$  pairing strength in QRPA is changed as a parameter  $f$ .

# Neutron-proton pair condensates

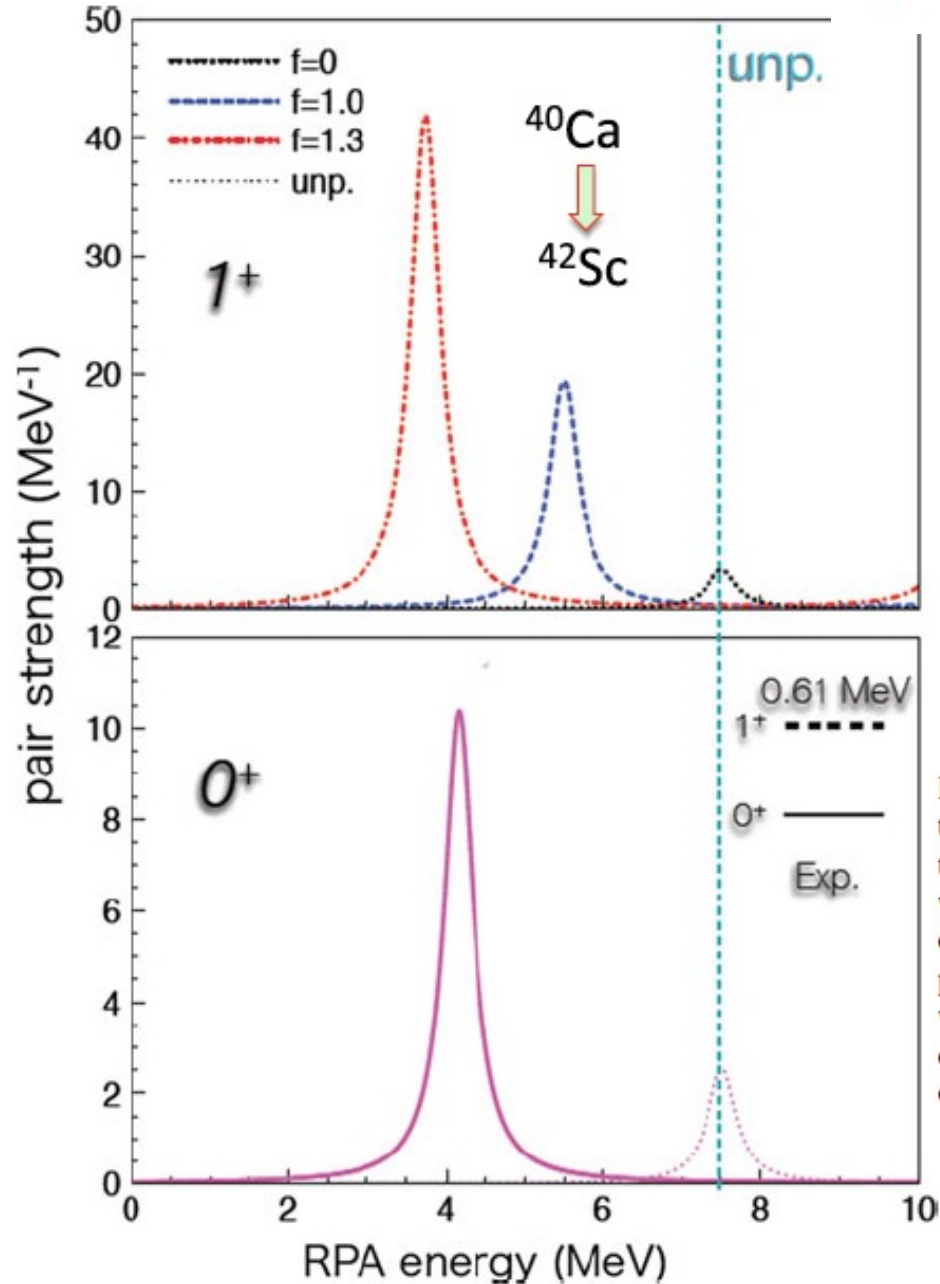
Gerzelis and Bertsch, PRL 106 (2011)



Source	$v_s$ (MeV fm <sup>3</sup> )	$v_t$ (MeV fm <sup>3</sup> )	Ratio
<i>sd</i> shell [8]	280	465	1.65
<i>fp</i> shell [9]	291	475	1.63

G.F. Bertsch and Y. Luo, PRC81, 064320 (2010)

$$P_{T=1,S=0}^{\dagger}(T=0,S=1) = \frac{1}{2} \int d\mathbf{r} [a^{\dagger}(\mathbf{r}\tau\sigma)a^{\dagger}(\mathbf{r}\tau'\sigma')]^{T=1,S=0(T=0,S=1)},$$



$$S_{\text{ad}} = \sum_{n \in A+2} |\langle n | P^{\dagger} | 0 \rangle|^2 \delta(E - E_n),$$

$$S_{\text{rm}} = \sum_{n \in A-2} |\langle n | P | 0 \rangle|^2 \delta(E - E_n),$$

Fig. 6.56 RPA results of  $L = 0$  neutron-proton pair addition strength (6.66) in the case of the transitions  $^{40}\text{Ca} \rightarrow ^{42}\text{Sc}$ . In the case of  $J^{\pi} = 1^{+}$  states the operator  $P_{T=0,S=1}$  is active, whereas in the case of  $J^{\pi} = 0^{+}$  states drawn by the purple line in the lower panel, the strength is associated with  $P_{T=1,S=0}$ . The sharp peaks associated with the strength function (6.66) are smeared by means of Lorentzian functions with a width of 0.1 MeV. In the  $(J, T) = (1, 0)$  channel the spin-triplet pairing strength is changed by scaling factors  $f \equiv v_t/v_s = 0.0, 1.0,$  and  $1.3$  [cf. Equation (6.64)] while the spin-singlet pairing is fixed. The unperturbed pair transfer strength is also shown by a dotted line. In the lower panel, the experimental level scheme is inserted. This figure is drawn based on the results in [32]. Courtesy K. Yoshida, Kyoto University



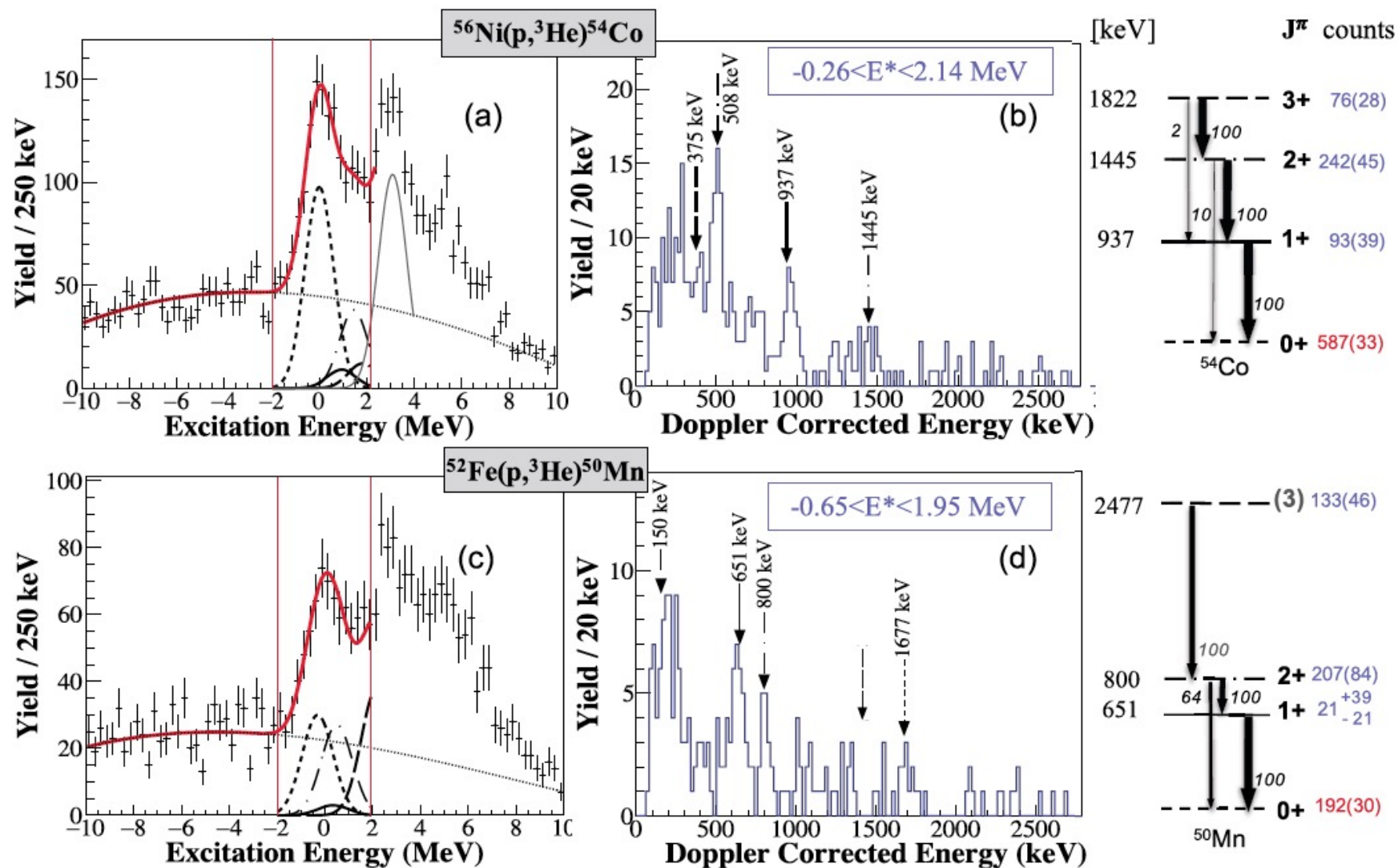


**Fig. 2.** (Left) Excitation energy spectra for  $^{56}\text{Ni}(p,^3\text{He})^{54}\text{Co}$  (a) and for  $^{52}\text{Fe}(p,^3\text{He})^{50}\text{Mn}$  (c). The background contribution deduced from the measurement on a  $^{12}\text{C}$  target is shown as a light dotted line (see text for details). (Right) The associated gamma spectra with a gate on the excitation energy centered on the first ( $J=1^+$ ,  $T=0$ ) state  $\pm 2\sigma$  (the gate in  $E^*$  is given explicitly on the spectra). A simplified level scheme of the residual nuclei is shown with the main transitions and associated intensities taken from [30]. The deduced direct feeding by the transfer reaction (in number of counts) of each excited state is shown in blue with its statistical error bars (see text for details). This information is used to constrain the fit of the excitation energy (shown as a thick red line on spectra a) and c)). The population of the ground state (given in red) is deduced from the fit. The contribution of each state to the fit is identified with the same line code as for the associated gamma-ray lines (dotted for the gs, full for the  $1^+$ , dashed dotted for the  $2^+$  and dashed for the  $3^+$  state). For  $^{56}\text{Ni}(p,^3\text{He})^{54}\text{Co}$  a contribution at higher energy (around 3 MeV) is also shown and detailed in the text.

**Table 1**

Theoretical (based on second-order DWBA calculations) and experimental cross-sections for  $^{56}\text{Ni}(p, ^3\text{He})$  and  $^{52}\text{Fe}(p, ^3\text{He})$ . For cross-sections, the first error bar given corresponds to the statistical one and the second one to the systematics errors. For the ratios, the error bar is only the statistical one (see text for details).

	$\sigma(0^+, T=1)$ ( $\mu\text{b}$ )	$\sigma(1^+, T=0)$ ( $\mu\text{b}$ )	Ratio
$^{56}\text{Ni}(p, ^3\text{He})^{54}\text{Co}$			
this work	$109^{stat}_{\pm 5} \ ^{sys}_{\pm 10}$	$17^{stat}_{\pm 7} \ ^{sys}_{\pm 2}$	$6.3^{+3.1}_{-2.1}$
SP	73	19	3.8
GXPF1	136	21	6.4
$^{52}\text{Fe}(p, ^3\text{He})^{50}\text{Mn}$			
this work	$145^{stat}_{\pm 12} \ ^{sys}_{\pm 15}$	$16^{+29}_{-16} \ ^{sys}_{\pm 2}$	$9.1^{+\infty}_{-3.7}$
SP	69	16	4.3
GXPF1	257	17	15.1

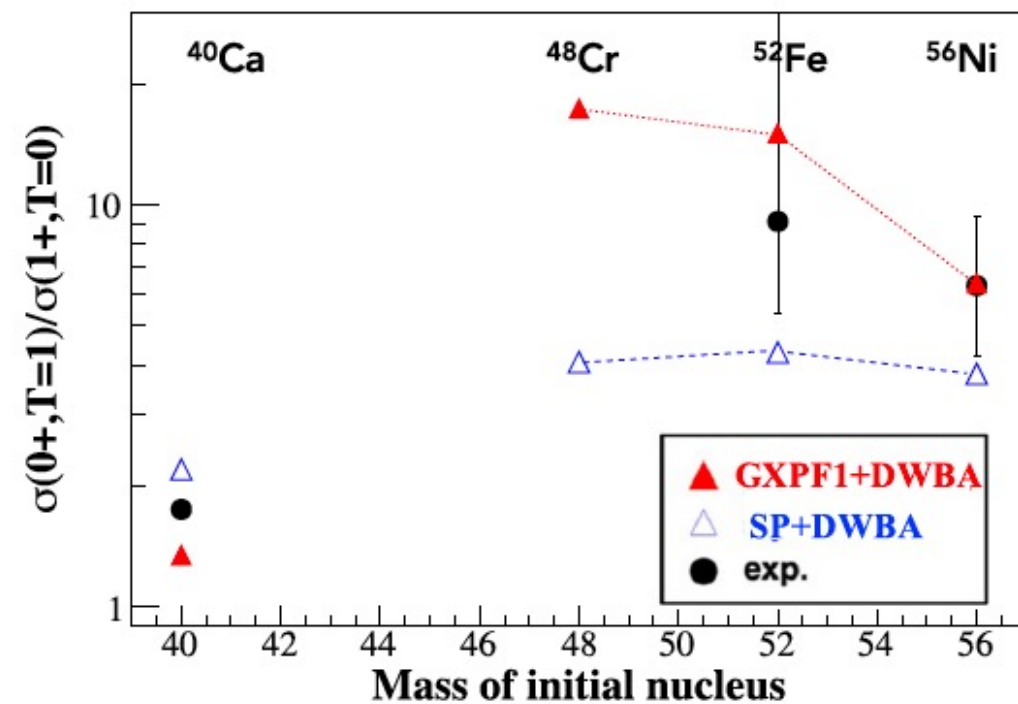


**Fig. 4.** Ratio  $\sigma(0^+, T=1)/\sigma(1^+, T=0)$  obtained in this experiment (black dots) and for second order DWBA calculations with GXPF1 (red triangle) and SP picture (blue squares).  $^{40}\text{Ca}$  results are taken from ref. [17].

T=1 S=0 pairing and T=0 S=1 pairing interactions

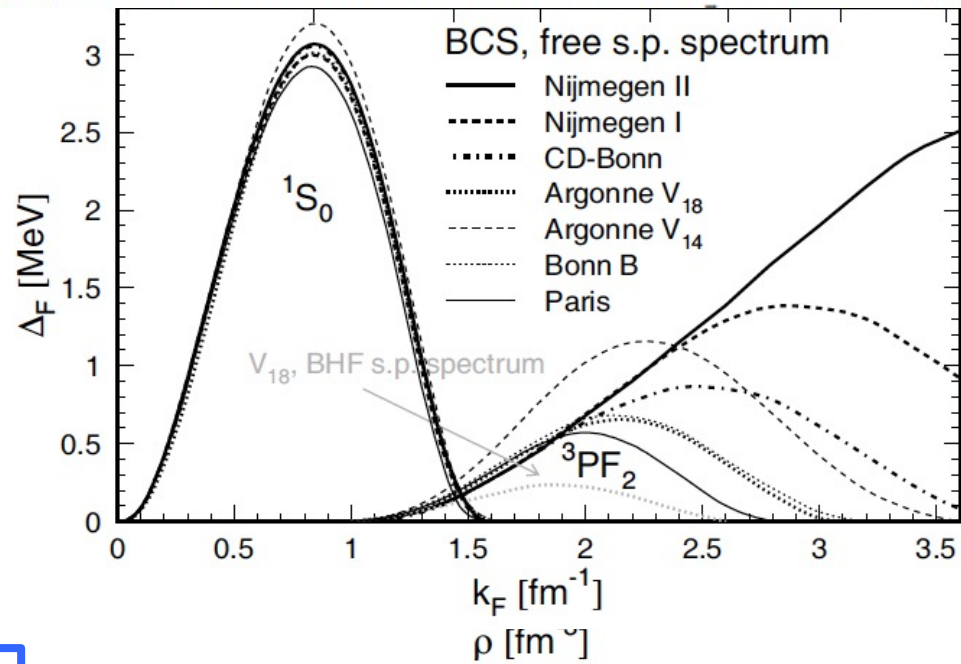
T=1 pairing (n-n, p-p pairing correlations) → spin singlet superfluid

- mass (odd-even staggering)
- energy spectra (gap between the first excited state and the ground state in even-even nuclei)
- moment of inertia
- n-n or p-p Pair transfer reactions
- fission barrier (large amplitude collective motion)

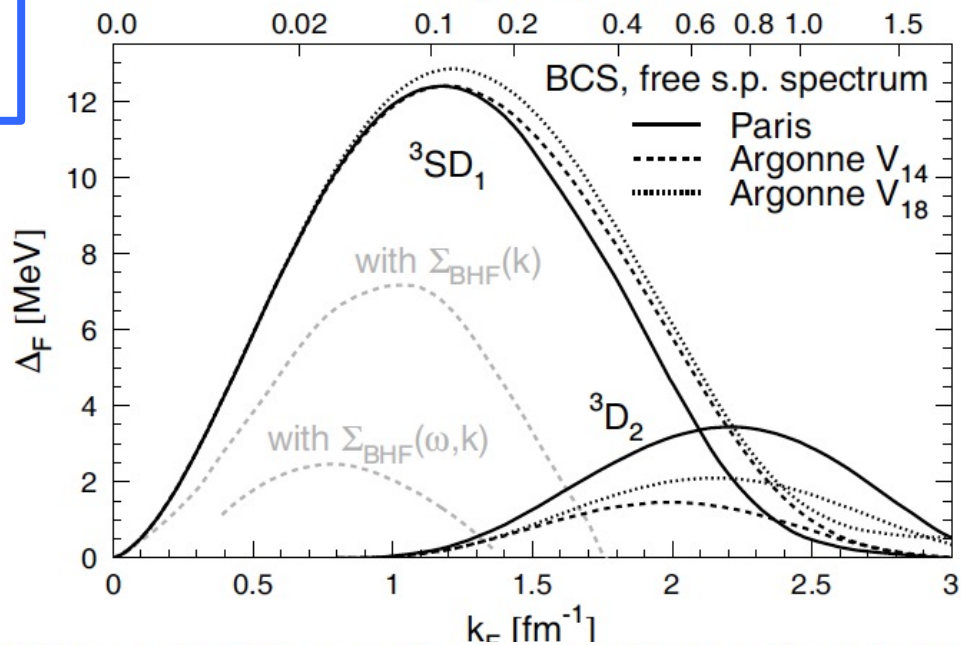
Strong T=0 pairing (p-n pairing with S=1) → spin triplet superfluid ?

- deuteron (T=0,S=1) is bound, but not di-neutron (T=1,S=0)
- N=Z Wigner energy (still controversial)
- Energy spectra in nuclei with N=Z (T=0 and J=1)
- n-p pair transfer reaction
- low-energy super-allowed Gamow-Teller transition in N=Z and N=Z+2 between SU(4) supermultiples
- Double-beta decay

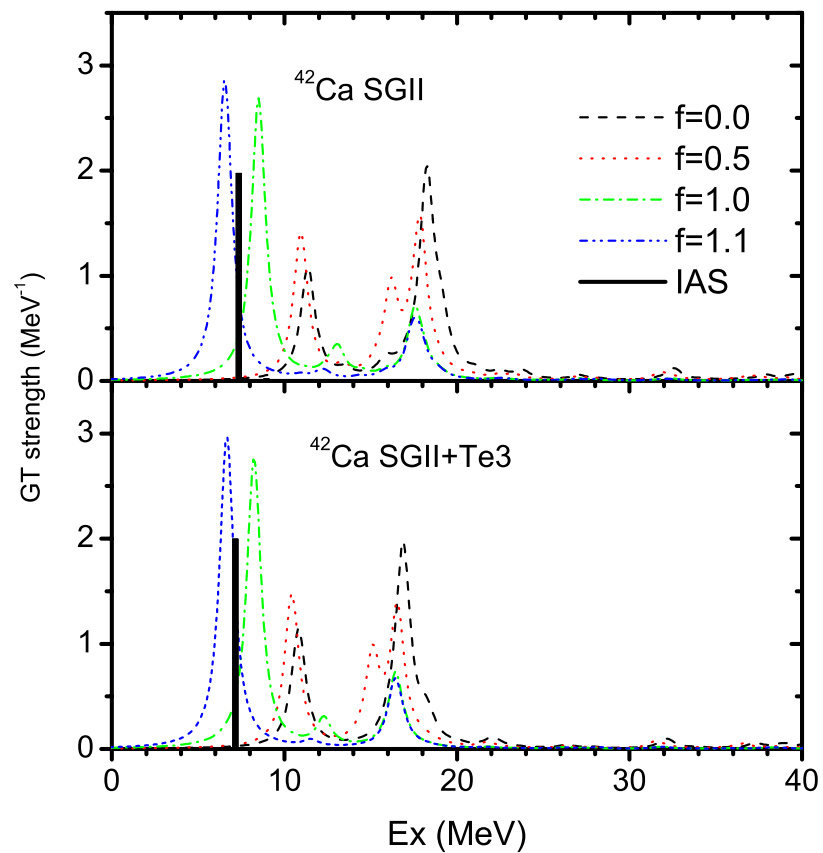
Isospin  $T = 1$   $^1S_0$  and  $^3PF_2$  gaps in neutron matter evaluated in BCS approximation



Int. Journ. of Mod. Phys.E14, 513 (2005)  
U. Lombardo et al..



Isospin  $T = 0$   $^3SD_1$  and  $^3D_2$  gaps in symmetric nuclear matter



Effect of tensor correlations is small in  $^{42}\text{Ca}$ .

